Effects of Various Physical and Numerical Parameters on Heat Transfer in Vertical Passages at Relatively Low Heat Loading

Amir Keshmiri

School of Mechanical, Aerospace and Civil Engineering (MACE), The University of Manchester, Manchester, M13 9PL, U.K.

Tel: +44 161 275 4401; fax: +44 161 306 3723
E-mail address: a.keshmiri@manchester.ac.uk

Abstract

The present work is concerned with the modelling of buoyancy-modified mixed convection flows, such flows being representative of low-flow-rate flows in the cores of Gas-cooled Reactors. Three different Eddy Viscosity Models (EVMs) are examined using the in-house code, 'CONVERT'. All fluid properties are assumed to be constant and buoyancy is accounted for within the Boussinesq approximation. Comparison is made against experimental measurements and the direct numerical simulations (DNS). The effects of three physical parameters including the heat loading, Reynolds number and pipe length on heat transfer have been examined. It is found that by increasing the heat loading, three thermal-hydraulic regimes of 'early-onset of mixed convection', 'laminarization', and 'recovery' were present. At different Reynolds numbers, the three thermal-hydraulic regimes are also evident. The k-ε model of Launder and Sharma was found to be in the closest agreement with consistently-normalized DNS results for the ratio of mixed-to-forced convection Nusselt number (Nu/Nu_0). It was also shown that for the 'laminarization' case, the pipe length should be at least '500×diameter' in order to reach a fully-developed solution. In addition, the effects of two numerical parameters namely Buoyancy production and Yap length-scale correction terms have also been investigated and their effects were found to be negligible on heat transfer and friction coefficient in ascending flows.

Key words: 'buoyancy-influenced flow', 'EVM', 'heat loading', 'mixed convection', 'RANS'.

1 Introduction

'Mixed' convection flows occur where both the regimes of 'forced' and 'free' convection operate simultaneously and there is a buoyancy-modified forced flow. In mixed convection

Axcell and Hall [11] carried out experiments on descending flow with nitrogen and air, respectively.

In the simulations reported in this paper, the focus is on the DNS of You et al. [12] who conducted a study of turbulent mixed convection in a vertical uniformly-heated pipe for constant property conditions; buoyancy was accounted for using the Boussinesq approximation. Adoption of the Boussinesq approximation framework is attractive from the viewpoint of turbulence model/computer code validation because it permits an examination of buoyancy effects in isolation from other variable property phenomena

Complementing experimental research in the area, numerical simulations of mixed convection flows have been reported by Abdelmeguid and Spalding [13], Tanaka et al. [14], Cotton and Jackson [15], Richards et al. [16], Kim et al. [17], Keshmiri et al. [18] and Billard et al. [19]who have used various forms of two-equation turbulence models. A finding to emerge from the studies taken together was that the 'low-Reynolds-number' model of Launder and Sharma [20] was generally superior to the other variants examined. Other turbulence models including the three-equation closure of Cotton and Ismael [21] and the 'v^2-f' model of Durbin [22] have also produced satisfactory results when applied to mixed convection flows [17]. In addition, in Keshmiri et al. [23] Large Eddy Simulations (LES) employing the classical Smagorinsky sub-grid-scale model were also presented and good agreement with the DNS data was obtained.

In the present work, buoyancy-influenced ascending and descending pipe flows are computed using three eddy viscosity turbulence models: 1) Launder-Sharma model [20], 'LS model', 2) Cotton-Ismael model [21], 'CI model' and 3) Craft et al. model [24], 'Suga model'. While they are all 'low-Reynolds-number' schemes, the CI and Suga closures also incorporate dependence on a 'strain parameter'. The effects of three physical parameters including the heat loading, Reynolds number and pipe length on heat transfer are examined. Further more, the effects of buoyancy production and Yap length-scale correction terms on heat transfer and friction

2 Physical and Numerical Formulation

2.1 Mean Flow Equations

The mean flow equations of continuity, momentum and energy are cast in the Boussinesq approximation:

$$\frac{\partial U_j}{\partial x_j} = 0 \tag{2}$$

$$U_j \frac{\partial U_i}{\partial x_j} = -\frac{1}{\rho}\frac{\partial p}{\partial x_i} + \frac{\partial}{\partial x_j}\left((\nu + \nu_t)\frac{\partial U_i}{\partial x_j}\right) + \left[1 - \beta(T - T_0)\right]g_i \tag{3}$$

where $g_i = -g$ in ascending and $g_i = +g$ in descending flows.

$$U_j \frac{\partial T}{\partial x_j} = \frac{\partial}{\partial x_j}\left[\left(\frac{\nu}{Pr} + \frac{\nu_t}{\sigma_t}\right)\frac{\partial T}{\partial x_j}\right] \tag{4}$$

where, following standard modelling practice, e.g. Launder and Sharma [20], the turbulent Prandtl number is set to a constant value, $\sigma_t = 0.9$.

2.2 Eddy-Viscosity Turbulence Models

The three turbulence models to be evaluated in the present study are as follows:

2.2.1 Launder and Sharma k-ε Model – 'LS Model'

In the present work, the *k-ε* model due to Launder and Sharma [20] is adopted as a benchmark against which more recent strategies are assessed. Despite the early appearance of the LS closure it remains one of the more conceptually advanced, and accurate, of a large group of two-equation model variants. The equations of the LS model and other 2-equation EVMs may be written in the following generic form:

$$-\overline{u_i u_j} = \nu_t\left(\frac{\partial U_i}{\partial x_j} + \frac{\partial U_j}{\partial x_i}\right) - \frac{2}{3}\delta_{ij}k \tag{5}$$

$$\frac{Dk}{Dt} = P_k + P_G + \frac{\partial}{\partial x_j}\left[\left(\nu + \frac{\nu_t}{\sigma_k}\right)\frac{\partial k}{\partial x_j}\right] - \left[\tilde{\varepsilon} + 2\nu\left(\frac{\partial (k)^{1/2}}{\partial x_j}\right)^2\right] \tag{6}$$

$$\frac{D\tilde{\varepsilon}}{Dt} = C_{\varepsilon 1}\frac{\tilde{\varepsilon}}{k}P_k + C_{\varepsilon 1}\frac{\tilde{\varepsilon}}{k}P_G + \frac{\partial}{\partial x_j}\left[\left(\nu + \frac{\nu_t}{\sigma_\varepsilon}\right)\frac{\partial \tilde{\varepsilon}}{\partial x_j}\right] - C_{\varepsilon 2} f_\varepsilon \frac{\tilde{\varepsilon}^2}{k} + E_\varepsilon + Y \tag{7}$$

where P_G and Y are the buoyancy production and Yap length-scale correction terms, respectively

2.2.3 Suga k-ε Model – 'Suga Model'

In a research effort that proceeded in parallel with the development of the CI model, Craft, Launder and Suga [24] developed a two-equation model in which quadratic and cubic mean strain and vorticity terms were introduced into the constitutive equation. The transport equations for k and ε in the Suga model take the generic forms of Eqs. (6) and (7); model constants and functions are given in Tables A1 and A2. It is noted that the strain field of the present mixed convection flows approximates simple shear and that the non-linear terms of the Suga model are consequently close to zero. The model does, however, depart significantly from the standard k-ε closure because of the specification of C_μ which has a parameterization akin to the $f_s(S)$ damping function of the CI model. An additional source term in the Suga model ε-equation which is generally referred to as the 'Yap correction' [24] has been omitted in the present work (the effects of including the Yap term will be discussed in Section 4.2.2 below).

2.3 Turbulent Heat Flux Modelling

In order to calculate heat transfer, the energy equation must be closed, i.e. a model for the turbulent heat fluxes are required. In the present work, in order to model the turbulent heat fluxes, $\overline{u_i\theta}$, two methods are used and are briefly described below:

2.3.1 Simple Gradient Diffusion Hypothesis (SGDH)

This approach to modelling the turbulent heat fluxes relies upon the concept of an isotropic turbulent thermal conductivity

$$\rho c_p \overline{u_i\theta} = -\lambda_t \frac{\partial T}{\partial x_i} \tag{10}$$

where

$$\overline{u_i\theta} = -\frac{\nu_t}{\sigma_t}\frac{\partial T}{\partial x_i} \tag{12}$$

Therefore, the buoyancy production term becomes

$$P_G = \beta\, g_i\, \frac{\nu_t}{\sigma_t}\frac{\partial T}{\partial x_i} \tag{13}$$

It is well known that in a simple shear flow with only wall-normal temperature variations, the heat flux in the streamwise direction is usually significantly larger than in the wall-normal direction. Therefore, in spite of λ_t being notionally isotropic, equations of the form of Eq. (10) may lead to a poor approximation to the axial turbulent heat flux since temperature variations are negligible in this direction [15].

2.3.2 Generalized Gradient Diffusion Hypothesis (GGDH)

This method which was first introduced by Daly and Harlow [26] may provide a better model for P_G in comparison to SGDH. In Generalized Gradient Diffusion Hypothesis (GGDH), the turbulent heat flux is modelled as

$$\overline{u_i\theta} = -c_\theta \frac{k}{\varepsilon}\overline{u_i u_j}\frac{\partial T}{\partial x_j} \tag{14}$$

where $c_\theta = 0.3$. Therefore, the buoyancy production term becomes

$$P_G = \beta\, g_i\, c_\theta \frac{k}{\varepsilon}\overline{u_i u_j}\frac{\partial T}{\partial x_j} \tag{15}$$

It has been reported by Cotton [27] that inclusion of P_G in the k and ε transport equations has an insignificant effect when modelled in accordance with the SGDH and only a second-order effect when modelled using the GGDH. The effects of including the Buoyancy production term and modelling the turbulent heat flux using both the SGDH and the GGDH are discussed further in Section 4.2.1 below.

3 Computational Code; CONVERT

The present computations have been performed using an in-house code, known as 'CONVERT' (for Convection in Vertical Tubes). CONVERT was originally developed by Cotton [27] and later extended by a number of researchers; the latest version which is used here is due to Keshmiri [18]. The code is written in the 'thin shear' (or 'boundary layer') approximation. The thin shear equations are of parabolic form and therefore the program is able to 'march' in the streamwise direction.

The radial mesh consists of 100 control volumes and the wall-adjacent node is typically located at $y^+ = 0.5$. A number of tests with different mesh refinement have been carried out to ensure grid independency prior to running the present computations. Interested readers are referred to [18, 23, 27] for further details on CONVERT.

4 Results and Discussion

4.1 Physical Parameters

4.1.1 Effects of the Heat Loading

Fig. 1 provides an overview of heat transfer performance in ascending and descending flow. Nusselt number in mixed convection, Nu is normalized by the corresponding forced convection value evaluated at the same Reynolds and Prandtl numbers using a re-optimized form of the Dittus-Boelter equation:

$$Nu_0 = 0.022\, Re^{0.8} Pr^{0.5} \tag{16}$$

In Fig. 1 Nu/Nu_0 is plotted against the buoyancy parameter, Eq. (1). Present turbulence model results are shown together with the ascending and descending flow DNS data of You et al. [12] and the experimental results of Steiner [5], Carr et al. [6] and Easby [10].

In their direct simulations You et al. adopted the Boussinesq approximation and cast the governing equations in fully-developed form. The Reynolds and Prandtl numbers of the seven

simulations (one forced convection and six mixed convection) were 5,300 and 0.71. (In the case of ascending flow, three simulations were reported by You et al. [12], each representing a different thermal-hydraulic regime, see Table 1.) By contrast, the three sets of experimental data all span a range of Reynolds number. It follows that some uncertainty is introduced into the comparisons because any functional dependence of Nu/Nu_0 on Bo is not exact. A second uncertainty is introduced because the experimental works do not report values for forced convection Nusselt number. Measured values of mixed convection Nusselt number are consequently normalized using Nu_0 determined from Eq. (16) (with $Pr = 0.71$).

An immediately striking feature of the ascending flow portion of Fig. 1 is the catastrophic onset of large-scale heat transfer impairment that occurs at $Bo \approx 0.2$. Examining the EVM results, it is seen that the LS model is in closest agreement with the direct simulation data; the CI model returns a similar minimum level of heat transfer, but indicates that this is attained at higher Bo. Significantly lower levels of heat transfer impairment are returned by the Suga model and the onset of impairment is delayed considerably. In the 'recovery' region ($Bo \geq 0.5$) the LS and CI models are in close agreement, but the Suga model yields lower Nu/Nu_0.

Consideration of the descending flow region of Fig. 1 reveals that there is little difference between the heat transfer enhancement levels of the Suga and CI models. The Nu/Nu_0 vs. Bo curve of the LS model lies above the other two EVM schemes, while the three DNS points suggest a lower trajectory.

4.1.2 Effects of the Reynolds Number

In this section, effects of varying the Reynolds number on heat transfer and friction coefficient are examined. Six Reynolds numbers are selected in a range between 5,000 and 25,000. At each Reynolds number, the Grashof number was varied (by changing the heat flux) so as to cover all four regimes in Table 1. The LS model been used to carry out the computations in this section.

Values of fully-developed forced convection Nusselt number (Nu_0) and friction coefficient (c_{f0}) at different Reynolds numbers are shown in Table 2. These values are compared against the modified form of the Dittus-Boelter equation (Eq. (16)) and the Blasius equation, i.e. $c_{f0} = 0.079\,Re^{-0.25}$. Compared to the correlations, the LS model under-estimates the Nusselt number and friction coefficient by an average of 2.2% and 8.7%, respectively. The under-prediction of c_f by the LS model is related to the under-prediction of the wall shear stress, since $c_f = \tau_w / (0.5\rho U_b^2)$.

In Fig. 2 normalized Nusselt number is plotted against the buoyancy parameter for different Reynolds numbers. In Fig. 2 it is seen that the general trend of the Nusselt number is broadly the same for different Reynolds numbers. A dramatic reduction in heat transfer levels is evident in all cases at around $0.15 < Bo < 0.2$, except for Re = 25,000 where the heat transfer impairment is not as sudden as in other cases. After the maximum impairment point, by increasing the buoyancy influence, the heat transfer levels enhance in proportion to approximately $Bo^{0.32}$.

In addition, it is seen that the original definition of Bo (Eq. (1)) results in collapsing curves of Nu/Nu_0 obtained at different Re in recovery region i.e. $Bo > 0.25$. It is, however, unable to produce a satisfactory collapse of the family of curves at lower levels of buoyancy influence (i.e. to the left of the maximum impairment point).

4.1.3 Effects of the Pipe Length

In this section, mean flow and turbulence profiles for the laminarized regime (case C; Bo =f0.18) obtained a

Fig. 3 are computed

= 0.71) using the La

ε model – see Fig. 3(a) and (b).

From Fig. 3, it is evident that the profiles demonstrate marked development effects. In Fig. 3(a) and (b), a series of minima and maxima are present for $x/D > 350$ which correspond to local recoveries in Nu– and c_f –developments. (Note that these oscillations are less evident in Fig. 3a

due to the scale of the y-axis.) Differences are also evident between the Nu– and c_f – developments which lead to a conclusion that in a buoyancy-influenced flow the relationship between momentum transfer and heat transfer is less direct than in forced convection [17].

In all the profiles shown in Fig. 3(c)-(f), it is seen that at x/D = 200 the profiles are quite similar to the profiles obtained for conditions at which buoyancy influence is low e.g. cases (A) and (B). At x/D = 300 and 350, however, the flow begins to laminarize, but it is only at x/D = 500 where the flow can be assumed to be fully-developed i.e. complete laminarization occurs.

From Fig. 3(c) and (d) it is seen that the velocity and temperature profiles at x/D = 350 and 500 are relatively close, however, there are rather large discrepancies in the profiles shown in Fig. 3(e) and (f). Such diverse performances of flow at different x/D show the importance of the pipe length (computational domain) in numerical simulations of this type. It is also clear that in ascending flows, the mean flow equations and turbulence models must be cast in a developing flow framework in order to capture the complex thermo-fluid development [15].

4.2 Numerical Parameters

4.2.1 Effects of Buoyancy Production Term

In buoyancy affected problems, the buoyancy production term (P_G) could be added to both k and ε transport equations. The buoyancy production term in accordance with the Boussinesq approximation is defined as

$$P_G = -\beta\, g_i\, \overline{u_i\theta} \tag{17}$$

In all the results presented so far, the buoyancy production term was not included in the k- and ε-transport equations. In this section, the effects of including this term when modelled using the Simple Gradient Diffusion Hypothesis (SGDH) and Generalized Gradient Diffusion Hypothesis (GGDH) are examined (see Section 2.3 for a description of the SGDH and GGDH).

Fig. 4 shows that the effects of including the buoyancy production term (modelled using both the SGDH and GGDH) are insignificant. The same is true for the friction coefficient (although

not shown here).

Furthermore, distribution of the buoyancy production term (P_G) for all four thermal-hydraulic regimes using the GGDH and SGDH are shown in Fig. 5(a) and (b), respectively. Also shown in Fig. 5(a) are the DNS data of You et al. [12]. From the DNS data, it is evident that for cases (A) and (B), the effect of buoyancy production term is negligible, while in laminarized and recovery conditions (cases C and D) the effect of P_G becomes more significant. The buoyancy production term modelled using the GGDH returns values that are comparable with the DNS data, although the production levels are under-predicted for cases (C) and (D). However, as shown in Fig. 5(b) when the turbulent heat flux is modelled using the SGDH, the magnitudes of the buoyancy production term become nearly three orders of magnitude smaller compared to the DNS data. In addition, in contrast to the DNS data, in Fig. 5(b) the maximum value of buoyancy production occur at the pipe centre-line (y/R = 1). As was discussed earlier in Section 2.3.1, the SGDH results in a poor approximation of $\overline{u\theta}$ since temperature variations are negligible in the streamwise direction.

4.2.2 Effects of Yap Term

In some buoyancy-affected problems such as turbulent flows in cavities, the results were found to be improved by including an additional source term to the ε-transport equation [28]. This source term which acts as a length-scale correction term, is known as the 'Yap term' [29] and is defined as

$$Y = \max\left[0.83\left(\frac{l}{l_e} - 1\right)\left(\frac{l}{l_e}\right)^2 \frac{\varepsilon^2}{k},\ 0 \right] \tag{18}$$

where $l = k^{3/2} / \varepsilon$ and $l_e = 2.55\, y$.

Note that the Yap term has not been included in the calculations presented so far. At this part of the study, a series of computations were carried out for an ascending flow for a range of buoyancy parameter using the LS model with the Yap term included in the ε-equation. Although

the results are not shown here for the sake of brevity, it was found that in ascending mixed convection flows, including the Yap term has no effects on heat transfer and friction coefficient. Generally, the Yap term becomes active when the predicted turbulent length-scale exceeds the equilibrium length-scale which is not the case in an ascending flow problem. In fact, Cotton and Jackson [15] carried out a test on the ascending flow 'Run N13' of Carr et al. [6] and found that *Nu* changed by only 0.3% in response to inclusion of the Yap term. Including the Yap term for descending flow computations, however, produces marked improvement in the degree of accord with the data due to limitations of the modelling of the ε-equation in the LS model [15].

5 Conclusions

Ascending and descending turbulent mixed convection pipe flows have been computed using the Launder-Sharma ('LS'), Cotton-Ismael ('CI') and Craft-Launder-Suga ('Suga') turbulence models. The effects of three physical parameters including the heat loading, Reynolds number and pipe length on heat transfer have been examined. In an ascending flow, it was found that by increasing the heat loading, three thermal-hydraulic regimes of 'early-onset of mixed convection', 'laminarization' and 'recovery' were present. Comparison with the DNS data of You et al. [12] showed that the LS model best captures the three thermal-hydraulic regimes in an ascending flow, which were also found to exist for a wide range of Reynolds number (Re = 5,000 – 30,000). It was shown that the original definition of Bo (Eq. (1)) results in collapsing curves of Nu/Nu_0 obtained at different Re in recovery region i.e. $Bo > 0.25$. It is, however, unable to produce a satisfactory collapse of the family of curves at lower levels of buoyancy influence.

In addition, mean flow and turbulence profiles at four different streamwise locations (x/D = 200, 300, 350 and 500) were compared for the laminarized case using the LS model. Wide variations were found between the profiles and it was shown that for this case, the pipe length should be at least 500D in order to reach a fully-developed solution.

Finally, with regard to numerical parameters, the effects of including the buoyancy production

term (when modelled using SGDH and GGDH) and Yap length-scale correction term were examined and they found to have negligible effects on the heat transfer and friction coefficient results in an ascending flow problem.

Acknowledgments

This work was carried out as part of the UK Engineering and Physical Sciences Research Council 'Towards a Sustainable Energy Economy' (TSEC) programme 'Keeping the Nuclear Option Open' (KNOO). The author is also pleased to acknowledge the value of discussions with his colleagues Dr. M.A. Cotton, Dr. Y. Addad and Professor D. Laurence.

Nomenclature

Bo	Buoyancy parameter, $8\times10^4\, Gr/(Re^{3.425}Pr^{0.8})$
c_f	Local friction coefficient
D	Pipe diameter
g_i	Acceleration due to gravity
Gr	Grashof number, $\beta g D^4 \dot{q}/(\lambda \nu^2)$
k	Turbulent kinetic energy, $\overline{u_i u_i}/2$
Nu	Nusselt number, $\dot{q}D/\lambda(T_w - T_b)$
$\dot{q}$	Wall heat flux
Re	Reynolds number, $U_b D/\nu$
Re_t	Turbulent Reynolds number, $k^2/(\nu\tilde{\varepsilon})$
S	Strain parameter
S_{ij}	Mean strain rate tensor, $\partial U_i/\partial x_j + \partial U_j/\partial x_i$
$\tilde{S}$	Non-dimensional strain rate, $k/\tilde{\varepsilon}\sqrt{1/2(S_{ij}S_{ij})}$
$\overline{u_j\theta}$	Turbulent heat flux tensor
U_τ	Friction velocity, $(\tau_w/\rho)^{1/2}$
y^+	Dimensionless distance from the wall, yU_τ/ν

Greek Symbols:

δ_{ij}	Kronecker delta
ε	Rate of dissipation of k
$\tilde{\varepsilon}$	Modified dissipation rate, $\varepsilon - 2\nu(\partial k^{1/2}/\partial x_i)^2$
λ	Thermal conductivity
μ_t	Turbulent viscosity, or LES sub-grid viscosity
τ_w	Wall shear stress

Ω_{ij} Mean vorticity tensor, $\partial U_i / \partial x_j - \partial U_j / \partial x_i$

$\tilde{\Omega}$ Non-dimensional vorticity, $k / \tilde{\varepsilon} \sqrt{1/2(\Omega_{ij}\Omega_{ij})}$

Additional symbols are defined in the text.

References

[1] Petukhov, B. S., and Polyakov, A. F., 1988, *Heat Transfer in Turbulent Mixed Convection*, Hemisphere, Bristol, PA, USA.

[2] Jackson, J. D., Cotton, M. A., and Axcell, B. P., 1989, "Studies of Mixed Convection in Vertical Tubes," Int. J. Heat Fluid Flow, 10, pp. 2-15.

[3] Jackson, J. D., 2006, "Studies of Buoyancy-Influenced Turbulent Flow and Heat Transfer in Vertical Passages," Keynote lecture, 13th Int. Heat Transfer Conference, 'IHTC13', Sydney, Australia.

[4] Hall, W. B., and Jackson, J. D., 1969, "Laminarization of a Turbulent Pipe Flow by Buoyancy Forces," ASME Paper, 69-HT-55.

[5] Steiner, A., 1971, "On the Reverse Transition of a Turbulent Flow under the Action of Buoyancy Forces," J. Fluid Mech., 47, pp. 503-512.

[6] Carr, A. D., Connor, M. A., and Buhr, H. O., 1973, "Velocity, Temperature and Turbulence Measurements in Air for Pipe Flow with Combined Free and Forced Convection," J. Heat Transfer, 95, pp. 445-452.

[7] Polyakov, A. F., and Shindin, S. A., 1988, "Development of Turbulent Heat Transfer over the Length of Vertical Tubes in the Presence of Mixed Air Convection," Int. J. Heat Mass Transfer, 31, pp. 987-992.

[8] Vilemas, J. V., Poškas, P. S., and Kaupas, V. E., 1992, "Local Heat Transfer in a Vertical Gas-Cooled Tube with Turbulent Mixed Convection and Different Heat Fluxes," Int. J. Heat Mass Transfer, 35, pp. 2421-2428.

[9] Shehata, A. M., and Mceligot, D. M., 1998, "Mean Turbulence Structure in the Viscous Layer of Strongly-Heated Internal Gas Flows. Measurements," Int. J. Heat Mass Transfer, 41, pp. 4297-4313.

[10] Easby, J. P., 1978, "The Effect of Buoyancy on Flow and Heat Transfer for a Gas Passing Down a Vertical Pipe at Low Reynolds Numbers," Int. J. Heat Mass Transfer, 21, pp. 791-801.

[11] Axcell, B. P., and Hall, W. B., 1978, "Mixed Convection to Air in a Vertical Pipe," Proc. 6th Int. Heat Transfer Conference, Paper MC-7, Toronto, Canada.

[12] You, J., Yoo, J. Y., and Choi, H., 2003, "Direct Numerical Simulation of Heated Vertical Air Flows in Fully Developed Turbulent Mixed Convection," Int. J. Heat Mass Transfer, 46, pp. 1613-1627.

[13] Abdelmeguid, A. M., and Spalding, D. B., 1979, "Turbulent Flow and Heat Transfer in Pipes with Buoyancy Effects," J. Fluid Mech., 94, pp. 383-400.

[14] Tanaka, H., Maruyama, S., and Hatano, S., 1987, "Combined Forced and Natural Convection Heat Transfer for Upward Flow in a Uniformly Heated Vertical Pipe," Int. J. Heat Mass Transfer, 30, pp. 165-174.

[15] Cotton, M. A., and Jackson, J. D., 1990, "Vertical Tube Air Flows in the Turbulent Mixed Convection Regime Calculated Using a Low-Reynolds-Number k-ε Model," Int. J. Heat Mass Transfer, 33, pp. 275-286.

[16] Richards, A. H., Spall, R. E., and McEligot, D. M., 2004, "An Assessment of Turbulence Models for Strongly-Heated Internal Gas Flows," Proc. 15th IASTED Int. Conf. on Modeling and Simulation, Marina Del Rey, California, USA.

[17] Kim, W. S., Jackson, J. D., and He, S., 2008, "Assessment by Comparison with DNS Data of Turbulence Models Used in Simulations of Mixed Convection," Int. J. Heat Mass Transfer, 51, pp. 1293-1312.

[18] Keshmiri, A., Addad, Y., Cotton, M. A., Laurence, D. R., and Billard, F., 2008, "Refined Eddy Viscosity Schemes and Large Eddy Simulations for Ascending Mixed Convection Flows," Proc. 4th Int. Symp. on Advances in Computational Heat Transfer, 'CHT08', Paper CHT-08-407, Marrakech, Morocco.
[19] Billard, F., Uribe, J. C., and Laurence, D., 2008, "A New Formulation of the v^2-f Model Using Elliptic Blending and Its Application to Heat Transfer Prediction," Proc. 7th Int. ERCOFTAC Symp. on Engineering Turbulence Modelling and Measurements 'ETMM7', Limassol, Cyprus, pp. 89-94.
[20] Launder, B. E., and Sharma, B. I., 1974, "Application of the Energy Dissipation Model of Turbulence to the Calculation of Flow near a Spinning Disc," Lett. Heat Mass Transfer, 1, pp. 131-138.
[21] Cotton, M. A., and Ismael, J. O., 1998, "A Strain Parameter Turbulence Model and Its Application to Homogeneous and Thin Shear Flows," Int. J. Heat Fluid Flow, 19, pp. 326-337.
[22] Durbin, P. A., 1991, "Near-Wall Turbulence Closure Modeling without Damping Functions," Theoret. Comput. Fluid Dynamics, 3, pp. 1-13.
[23] Keshmiri, A., Cotton, M. A., Addad, Y., Rolfo, S., and Billard, F., 2008, "RANS and LES Investigations of Vertical Flows in the Fuel Passages of Gas-Cooled Nuclear Reactors," Proc. 16th ASME Int. Conf. on Nuclear Engineering, 'ICONE16', Paper ICONE16-48372, Orlando, Florida, USA.
[24] Craft, T. J., Launder, B. E., and Suga, K., 1996, "Development and Application of a Cubic Eddy-Viscosity Model of Turbulence," Int. J. Heat Fluid Flow, 17, pp. 108-115.
[25] Launder, B. E., and Spalding, D. B., 1974, "The Numerical Computation of Turbulent Flows," Comp. Meth. in Appl. Mech. Eng., 3, pp. 269-289.
[26] Daly, B. J., and Harlow, F. H., 1970, "Transport Equations in Turbulence," Phvsics Fluids, 13, pp. 2634-2649.
[27] Cotton, M. A., 1987, "Theoretical Studies of Mixed Convection in Vertical Tubes," Ph.D. thesis, Dept. of Engineering, University of Manchester, UK.
[28] Ince, N. Z., and Launder, B. E., 1989, "On the Computation of Buoyancy-Driven Turbulent Flows in Rectangular Enclosures," Int. J. Heat Fluid Flow, 10, pp. 110-117.
[29] Yap, C. R., 1987, "Turbulent Heat and Momentum Transfer in Recirculating and Impinging Flows," Ph.D. thesis, Dept. of Mech. Engineering, Faculty of Technology, UMIST (now the University of Manchester), UK.

Appendix

Table A1 compares the turbulence models of Launder-Sharma, Cotton-Ismael and Suga while Tables A1 and A2 show the coefficients appearing in these models.

List of Tables

List of Figures

Tables

Case	Bo	Thermal-Hydraulic Regime
A	0	Forced convection
B	0.13	Early-onset mixed convection
C	0.18	Laminarization
D	0.50	Recovery

Table 1. DNS cases of You et al. [12] in ascending flows.

Re	**Nu_0**	**0.022 $Re^{0.8}$ $Pr^{0.5}$**	**% diff.**	**c_{f0}**	**0.079 $Re^{-0.25}$**	**% diff.**
5,000	16.69	16.90	-1.2	8.69×10^{-3}	9.39×10^{-3}	-7.5
7,500	22.97	23.37	-1.7	7.75×10^{-3}	8.49×10^{-3}	-8.7
10,000	28.81	29.42	-2.1	7.18×10^{-3}	7.90×10^{-3}	-9.1
12,500	34.34	35.17	-2.4	6.78×10^{-3}	7.47×10^{-3}	-9.2
15,000	39.64	40.69	-2.6	6.49×10^{-3}	7.14×10^{-3}	-9.2
25,000	59.33	61.24	-3.1	5.75×10^{-3}	6.28×10^{-3}	-8.5

Table 2. Results for fully-developed forced convection using the Launder-Sharma model at different Reynolds numbers.

Variable	Launder-Sharma model	Cotton-Ismael model	Suga model
$\overline{u_i u_j}$ §	$-\nu_t\left(\frac{\partial U_i}{\partial x_j}\right)$	$-\nu_t\left(\frac{\partial U_i}{\partial x_j}\right)$	$(2/3)k\delta_{ij}-\nu_t S_{ij}+c_1\nu_t\frac{k}{\varepsilon}(S_{ik}S_{jk}-1/3S_{kl}S_{kl}\delta_{ij})$ $+c_2\nu_t\frac{k}{\varepsilon}(\Omega_{ik}S_{kj}+\Omega_{jk}S_{ki})$ $+c_3\nu_t\frac{k}{\varepsilon}(\Omega_{ik}\Omega_{jk}+1/3\Omega_{ik}\Omega_{ik}\delta_{ij})$ $+c_4\nu_t\frac{k^2}{\varepsilon^2}(S_{ki}\Omega_{lj}+S_{kj}\Omega_{li})S_{kl}$ $+c_5\nu_t\frac{k^2}{\varepsilon^2}(\Omega_{il}S_{mj}+S_{il}\Omega_{mj}-2/3S_{lm}\Omega_{mn}\delta_{ij})\Omega_{lm}$ $+c_6\nu_t\frac{k^2}{\varepsilon^2}S_{ij}S_{kl}S_{kl}+c_7\nu_t\frac{k^2}{\varepsilon^2}S_{ij}\Omega_{kl}\Omega_{kl}$
C_μ ‡	0.09	0.09	$\frac{0.3}{1+0.35\left(\max(\tilde{S},\tilde{\Omega})\right)^{1.5}}\times$ $\left(1-\exp\left[\frac{-0.36}{\exp\left(-0.75\max(\tilde{S},\tilde{\Omega})\right)}\right]\right)$
f_μ ‡	$\exp\left[-3.4/\left(1+\frac{Re_t}{50}\right)^2\right]$	$1-0.3\exp\left[\frac{-Re_t}{50}\right]$	$1-\exp\left[-(Re_t/90)^{1/2}-(Re_t/400)^2\right]$
f_S ‡	1	$\frac{2.88}{1+0.165S}\times$ $\left\{1-0.55\ e^{\left[-\left(0.135S+0.0015S^3\right)\right]}\right\}$	1
f_ε †	$1-0.3\exp\left(-Re_t^2\right)$	1	$1-0.3\exp\left(-Re_t^2\right)$
E_ε †	$2\nu\nu_t\left(\frac{\partial^2 U_i}{\partial x_j\partial x_k}\right)^2$	$0.9\nu\nu_t\left(\frac{\partial^2 U_i}{\partial x_j\partial x_k}\right)^2$	$0.0022\frac{\tilde{S}\nu_t k^2}{\tilde{\varepsilon}}\left(\frac{\partial^2 U_i}{\partial x_j\partial x_k}\right)^2$

* $\frac{Dk}{Dt}=P_k+\frac{\partial}{\partial x_j}\left[\left(\nu+\frac{\nu_t}{\sigma_k}\right)\frac{\partial k}{\partial x_j}\right]-\left(\tilde{\varepsilon}+2\nu\left(\frac{\partial (k)^{1/2}}{\partial x_j}\right)^2\right)$

† $\frac{D\tilde{\varepsilon}}{Dt}=C_{\varepsilon 1}\frac{\tilde{\varepsilon}}{k}\left(P_k+P_k'\right)+\frac{\partial}{\partial x_j}\left[\left(\nu+\frac{\nu_t}{\sigma_\varepsilon}\right)\frac{\partial\tilde{\varepsilon}}{\partial x_j}\right]-C_{\varepsilon 2}f_\varepsilon\frac{\tilde{\varepsilon}^2}{k}+E_\varepsilon$

‡ $\nu_t=C_\mu f_\mu f_S\frac{k^2}{\varepsilon}$

§ $P_k=-\overline{u_i u_j}\left(\partial U_i/\partial x_j\right)$

Table A1. Functions appearing in the LS, CI and Suga turbulence models.

Constants	LS model	CI model	Suga model
σ_k	1.0	1.0	1.0
σ_ε	1.3	1.21	1.3
$C_{\varepsilon 1}$	1.44	1.44	1.44
$C_{\varepsilon 2}$	1.92	1.92	1.92
σ_s	-	6.00	-

Table A2. Constants appearing in the LS, CI and Suga models.

c_1	c_2	c_3	c_4	c_5	c_6	c_7
-0.1	0.1	0.26	$-10\ C_\mu^{\ 2}$	0	$-5\ C_\mu^{\ 2}$	$5\ C_\mu^{\ 2}$

Table A3. Constants appearing in the Reynolds shear stress equation of the Suga model.

Figure

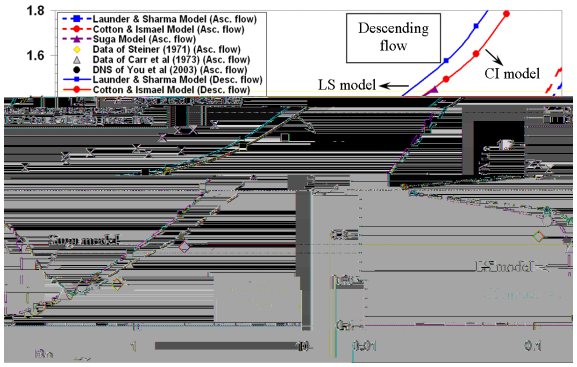

Fig. 1. Heat transfer impairment and enhancement in ascending and descending mixed convection flows (Re = 5,300; Pr = 0.71).

Author's comment: If space allows, Fig. 1 should be printed to fit half a page to become clearer for the reader.

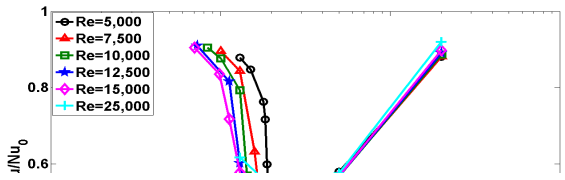

Fig. 2. Normalized Nusselt number impairment and enhancement against the buoyancy parameter for different Reynolds numbers.

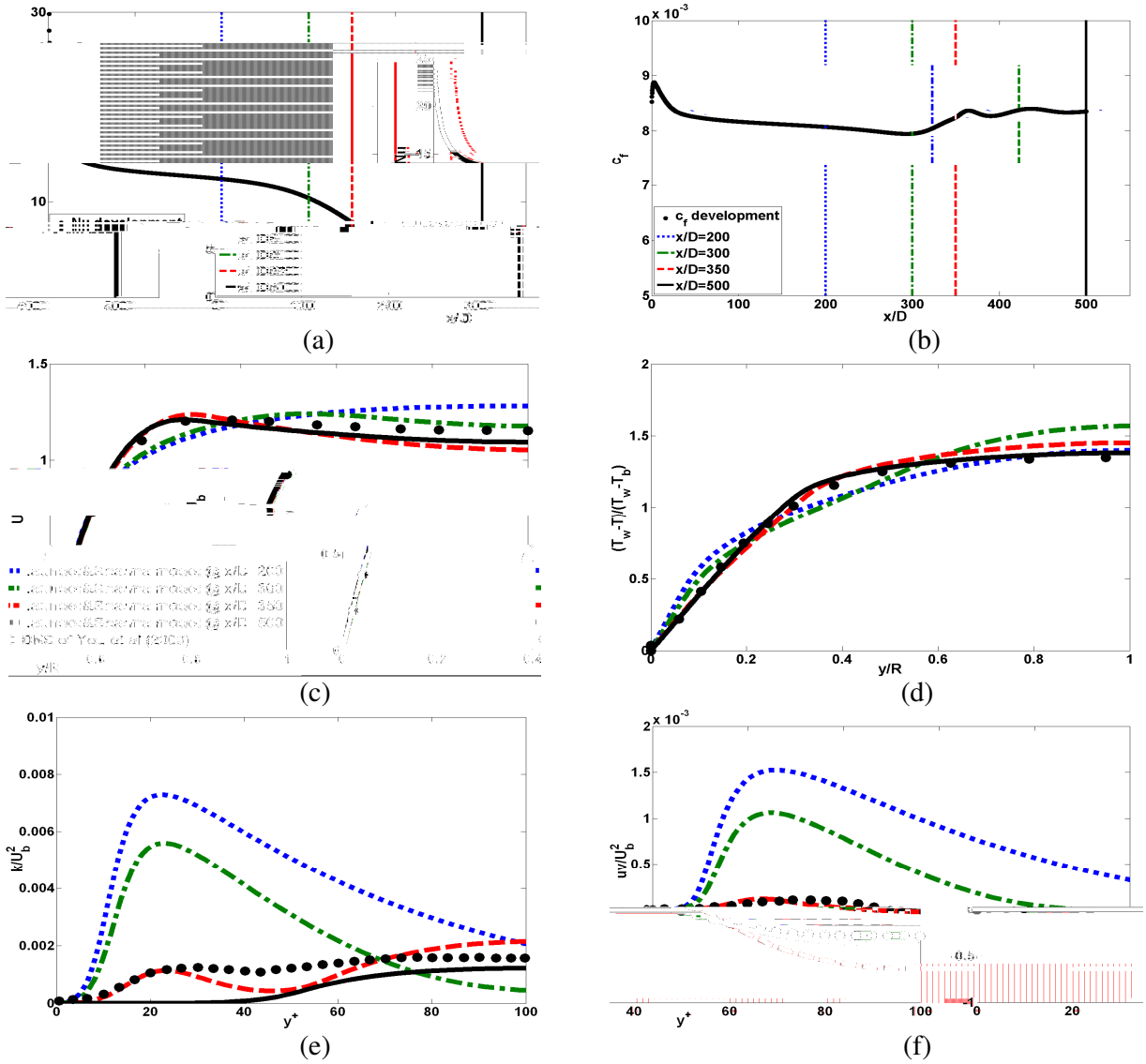

Fig. 3. Mean flow and turbulence profiles for case (C) at different streamwise locations obtained using the Launder-Sharma model in CONVERT.

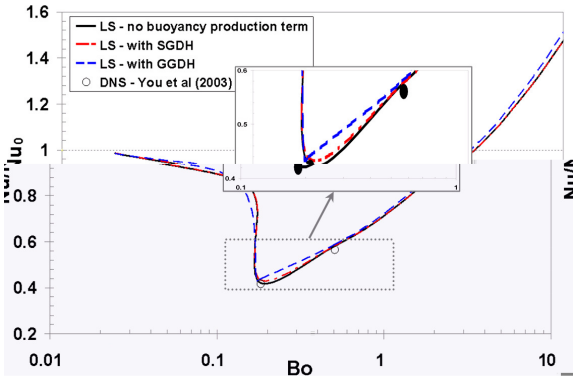

Fig. 4. Effects of including the buoyancy production term on the heat transfer impairment/enhancement.

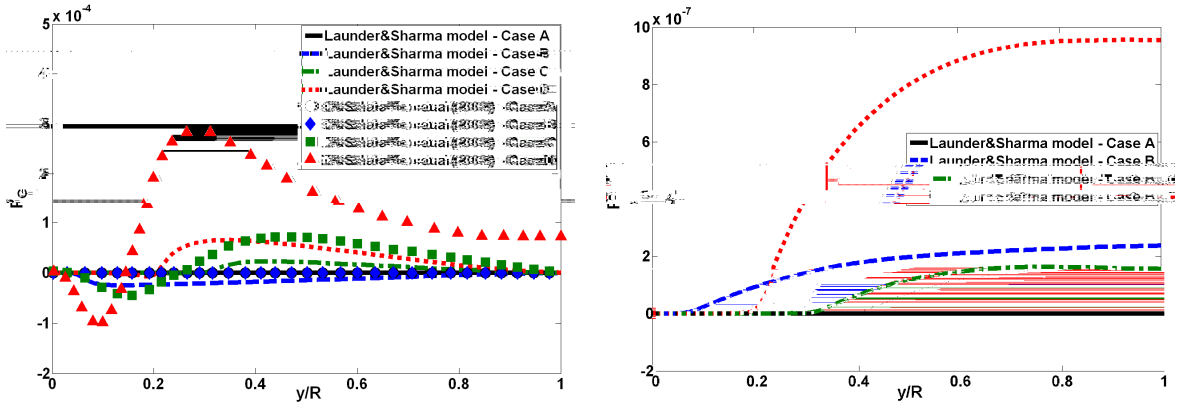

(a) (b)

Fig. 5. Effects of the heat flux models on the buoyancy production term [m^2/s^3] using (a) GGDH and (b) SGDH.